Monthly Notices of the ROYAL ASTRONOMICAL SOCIETY

MNRAS **470,** 2212–2224 (2017) doi:10.1093/mnras/stx1355
Advance Access publication 2017 June 6

CXO J004318.8+412016, a steady supersoft X-ray source in M 31

Marina Orio,[1,2★] G. J. M. Luna,[3,4,5★] R. Kotulla,[1] J. S. Gallager,[1] L. Zampieri,[2] J. Mikolajewska,[6] D. Harbeck,[7] A. Bianchini,[8] E. Chiosi,[8] M. Della Valle,[9,10] D. de Martino,[9] A. Kaur,[11] M. Mapelli,[2] U. Munari,[2] A. Odendaal,[12] G. Trinchieri,[13] J. Wade[1] and P. Zemko[8]

[1]*Department of Astronomy, University of Wisconsin, 475 N. Charter Str., Madison, WI 53704, USA*
[2]*INAF–Osservatorio di Padova, vicolo dell' Osservatorio 5, I-35122 Padova, Italy*
[3]*Universidad de Buenos Aires, Facultad de Ciencias Exactas y Naturales, Buenos Aires, Argentina*
[4]*CONICET-Universidad de Buenos Aires, Instituto de Astronomía y Física del Espacio (IAFE), Av. Inte., Güiraldes 2620, C1428ZAA, Buenos Aires, Argentina*
[5]*Universidad Nacional Arturo Jauretche, Av. Calchaquí 6200, F. Varela, Buenos Aires, Argentina*
[6]*N. Copernicus Astronomical Center, Polish Academy of Sciences, Bartycka 18, PL 00-716 Warsaw, Poland*
[7]*WIYN Observatory, Tucson, AZ 85719, USA*
[8]*Dipartimento di Astronomia, Università di Padova, vicolo Osservatorio, 2, 35122 Padova, Italy*
[9]*INAF-Osservatorio Astronomico di Capodimonte, Salita Moiariello 16, I-80131 Napoli*
[10]*International Center for Relativistic Astrophysics, Piazzale della Repubblica, 2, 65122, Pescara, Italy*
[11]*Department of Physics and Astronomy, Clemson University, Clemson, SC 29634, USA*
[12]*Department of Physics, University of the Free State, PO Box 339, Bloemfontein 9300, South Africa*
[13]*INAF–Osservatorio Astronomico di Brera, via Brera 28, 20121 Milano, Italy*

Accepted 2017 May 26. Received 2017 May 18; in original form 2016 December 31

ABSTRACT

We obtained an optical spectrum of a star we identify as the optical counterpart of the M31 *Chandra* source CXO J004318.8+412016, because of prominent emission lines of the Balmer series, of neutral helium, and a He II line at 4686 Å. The continuum energy distribution and the spectral characteristics demonstrate the presence of a red giant of K or earlier spectral type, so we concluded that the binary is likely to be a symbiotic system. CXO J004318.8+412016 has been observed in X-rays as a luminous supersoft source (SSS) since 1979, with effective temperature exceeding 40 eV and variable X-ray luminosity, oscillating between a few times 10^{35} erg s^{-1} and a few times 10^{37} erg s^{-1} in the space of a few weeks. The optical, infrared and ultraviolet colours of the optical object are consistent with an an accretion disc around a compact object companion, which may be either a white dwarf or a black hole, depending on the system parameters. If the origin of the luminous supersoft X-rays is the atmosphere of a white dwarf that is burning hydrogen in shell, it is as hot and luminous as post-thermonuclear flash novae, yet no major optical outburst has ever been observed, suggesting that the white dwarf is very massive ($m \geq 1.2$ M$_\odot$) and it is accreting and burning at the high rate $\dot{m} > 10^{-8}$ M$_\odot$ yr^{-1} expected for Type Ia supernovae progenitors. In this case, the X-ray variability may be due to a very short recurrence time of only mildly degenerate thermonuclear flashes.

Key words: binaries: symbiotic – white dwarfs – galaxies: individual: M31 – X-rays: binaries – X-rays: individual: CXO J004318.8+412016.

1 INTRODUCTION

Very luminous and persistent supersoft sources (SSS) have been observed since the end of the 1970s with the *Einstein* satellite, but they still pose an unsolved riddle. 60 per cent or more of the SSS are transient sources, and we know that the vast majority of these are post-outburst novae. In novae, the white dwarf (WD) keeps on burning hydrogen for a period of time ranging from a week to years after the outburst, with an atmospheric temperature of up to a million K. This has been clearly demonstrated in the Galaxy (see reviews by Orio 2012; Osborne 2015) and in the large SSS population of M31 (Pietsch, Freyberg & Haberl 2005; Orio 2006; Pietsch et al. 2006; Orio et al. 2010; Henze et al. 2014a,b).

However, the nature of numerous SSS is not yet understood, even if they may hold the key to outstanding astrophysical problems.

★ E-mail: orio@astro.wisc.edu (MO); gjmluna@iafe.uba.ar (GJML)

Because of their large intrinsic luminosity, these sources are observed in the direction of external galaxies, in the Local Group and beyond, up to a distance of 15 Mpc, in regions of the sky affected by low absorption. 1638 SSS are included in the last *Chandra* source catalog of X-ray sources (Wang et al. 2016). It is very likely that the majority of SSS are intrinsic in the population of the galaxies towards which they are observed; in fact, only 1 SSS out of $\simeq$100 in M31 has been found to be an active galactic nucleus in the background of the galaxy (Orio 2006; Orio et al. 2010, and references therein). Some objects in the low luminosity and high hardness-ratio end of the SSS in the Local Group are supernova remnants, but they do not constitute the majority of the observed SSS. We know now that many SSS that are persistently X-ray luminous defy a straightforward classification; this is especially true for the intriguing ones observed in galaxies outside the Local Group, whose luminosity appears to be super-Eddington for a star of a few solar masses (see Liu 2011; Liu et al. 2015). Recently Liu et al. (2015) have shown that a very luminous SSS, which is persistently supersoft and emitting at above-Eddington level for a stellar object, is most likely a micro-quasar hosting a stellar black hole.

Many SSS have been proven to be close binaries hosting the hottest, most massive accreting and hydrogen burning WDs, which may be on the verge of Type Ia supernova explosions (SNe Ia; see reviews by Orio 2012, 2013). Such WDs represent a key to understanding binary evolution and its endpoints. Perhaps, by revealing the nature of additional SSS, whether they are accreting and burning WDs or not, and by obtaining definite statistics, we will be able to better calibrate SNe Ia for cosmological purposes; we may find in fact whether there are different types of progenitors, causing deviations from the Phillips relationship at low metallicity (see e.g. Meng & Yang 2011). The models predict that, at very high mass transfer rate $\dot{m}$, the CNO-cycle hydrogen burning on the surface of a WD proceeds at such a high rate that all energy is irradiated (e.g. Fujimoto 1982; Wolf et al. 2013). When the most massive, hottest WDs do not undergo thermonuclear flashes causing nova outbursts, they accrete quietly until either a final explosion in a thermonuclear supernova, or a collapse to neutron star.

Following Luna et al. (2013), we define symbiotic stars as interacting binaries with a red giant, an asymptotic giant branch star, or exceptionally a supergiant, and a compact object of any nature. In the following context we will refer to WD-symbiotics as such (as opposed to rare symbiotics containing a neutron star or a black hole). In the Galaxy, in the Magellanic Clouds and in the Draco dwarf spheroidal galaxy, several WD-symbiotics host hydrogen burning WDs (Orio 2013, and references therein). However all of them but one, SMC 3, emit at the low end of the SSS effective temperature range, $T_{\rm eff} \leq 200\,000$ K, which is characteristic of low-mass WDs (see Starrfield et al. 2012; Wolf et al. 2013). Since the duration of the residual hydrogen burning phase is inversely dependent on $T_{\rm eff}$ and WD mass (see Section 3), and low-mass WDs may have a very long post-outburst residual hydrogen burning phase, it is still unclear whether some of these SSS WD-symbiotics are post-thermonuclear runaway novae, or whether they are really burning without ever ejecting and losing accreted mass.

In contrast with the relatively rich statistics of SSS WD-symbiotics, the census of persistent SSS binaries proven to host a main sequence companion and a WD still amounts to only two objects, CAL 83 and SMC 13, which have both been monitored for over 30 years. The latter hosts a low-mass WD and is not a Type Ia supernova candidate (Orio 2013, and references therein), but the WD of CAL 83 must be very massive (Lanz et al. 2005). There is some evidence that another very luminous SSS in M31, *Chandra* source CXO J004252.5+411539 or r2-12, may be a very short period binary (Chiosi et al. 2014).

In this article we present the optical spectrum of yet another very luminous and hot SSS in M31, the *Chandra* source CXO J004318.8+412016 (also cataloged as r3-8, as ROSAT source RX J0043.3+4120, and as *XMM–Newton* source 2XMM J004318.8+412017). This source was first detected in 1979 with *Einstein* (Trinchieri & Fabbiano 1991) and has been detected repeatedly in the last 28 yr in many exposures taken with *ROSAT*, *Chandra*, *Swift* and *XMM–Newton* (see Orio et al. 2010; Chiosi et al. 2014, and references therein). The optical spectrum is presented in Section 2. The source X-ray luminosity undergoes large fluctuations within months; we study and discuss the X-ray variability in Section 3. Section 4 presents a discussion of the results and we draw conclusions in Section 5.

2 THE GEMINI SPECTRUM

CXO J004318.8+412016 has an optical counterpart, a 22nd magnitude H$\,\alpha$ emitter (Massey et al. 2006; Hofmann et al. 2013; Chiosi et al. 2014). The coordinates of this object in the PHAT survey (Panchromatic Hubble Andromeda Treasury; Dalcanton et al. 2012) are $\alpha(2000) = 00{,}43{,}18.883$ and $\delta(2000) = +41{,}20{,}17.02$. This position differs from 0.52 arcsec from the *Chandra* HRC position determined by Kaaret (2002), 0.38 arcsec from the *Chandra* ACIS-S position determined by Barnard et al. (2014), 0.18 arcsec from the *XMM–Newton* 3XMM-DR6 catalog position (Rosen 2016) and 0.23 arcsec from the Swift coordinates of the 1SXPS catalog (Evans et al. 2013). In order to evaluate the spatial error box in which we may find the optical counterpart, we refer to the online handbooks of *Chandra* (the X-ray telescope with the best combination of pointing accuracy and spatial resolution) and of the *Hubble Space Telescope* (*HST*). The *Chandra* absolute astrometry is accurate to 0.63 arcsec at the 90 per cent confidence level, moreover Kaaret (2002) obtains an alignment with 2MASS sources with at most only a 0.4 arcsec discrepancy; the *HST* positions are generally accurate within 0.3 arcsec within the 90 per cent confidence level, but the PHAT astrometry should be even accurate to about 0.2 arcsec (Dalcanton et al. 2012). At the 90 per cent confidence level, using the nominal (handbook defined) spatial errors boxes of *HST* and the *Chandra* HRC-I (0.63 and 0.3 arcsec), our spatial error box is of 0.7 arcsec at the 90 per cent confidence level.

Several optical objects with magnitude between 25 and 27 in the blue *F*475*W* filter are detected in the PHAT within 0.7 arcsec; however, as we discuss in detail below, we did not find evidence of other emission lines emitters, as expected for the optical counterpart of an X-ray binary. The chance of finding an emission line star in a 0.7 arcsec error box is of course very small, probably less than 1 per cent, so our H$\,\alpha$ emitter is very likely to be one and the same with the X-ray source. Moreover, we do not expect a very faint optical counterpart, because the luminous X-ray source is powered either by accretion luminosity in a binary, or by hydrogen or helium burning, which must also be fueled by accretion at high rate (see the discussion on accretion luminosity in Chiosi et al. 2014). The large soft X-ray flux, the extreme softness of the X-ray spectrum and the X-ray variability pattern discussed below also suggest that the source, most likely, is not a background AGN. To summarize, we suggest that there is an extremely high probability that the target of our optical observation is one and the same with the X-ray source.

We observed our target with Gemini-North and the GMOS spectrograph in a queue mode (Observing Program GN-2015B-Q-56, PI: J.G.Luna) during the nights of 2015-08-20, 2015-08-26 and

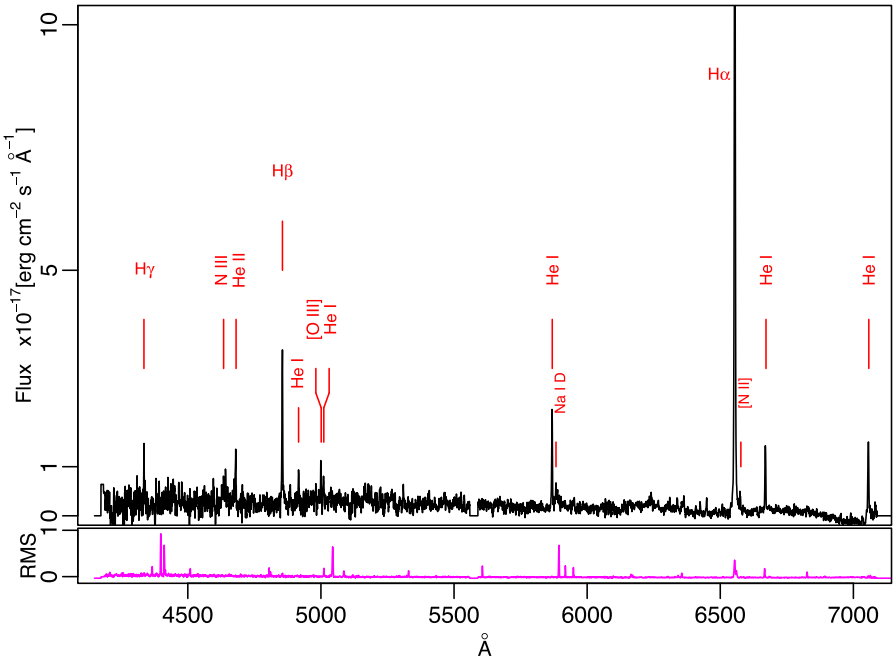

Figure 1. Median spectrum obtained with a stack of 10 exposures of the SSS binary CXO J004318.8+412016 in M31, obtained with the Gemini North telescope and the GMOS spectrograph. The purple line shows the root mean square error, indicating the deviation from the median of the stacked spectra. the peak of the Hα line is close to 14×10^{-17} erg cm^{-2} s^{-1} Å^{-1}, but we have cut the *y*-axis to allow seeing more detail in the other lines.

2015-09-12. A total of 10 science exposures, each with an exposure time of 1650 s, in a long-slit mode, using a 0.75 arcsec slit and the B600 grating centred on 5600/5650 Å, were obtained and used for the data analysis presented here. The observing conditions during the observations were photometric, with seeing <0.75 arcsec and dark skies. The spectrum was binned with a 2×2 binning in both spectral and spatial direction, and the spectral resolving power was $R = 1700$. The resulting median spectrum is shown in Fig. 1.

The data reduction and spectra extraction were done using a custom semi-automatic python script[1] following the standard Gemini/GMOS data reduction script. Each frame was corrected for bias and dark-current using the archive-provided master calibration products, and flat-fielded with the flat-field frames taken along with the science frames. The wavelength calibration was performed by means of Cu–Ar arc lamp spectra taken after each set of science frames, with spectrograph settings identical to that of the science frames. Each frame was also cleaned of cosmic ray hits using the appropriate setting in the `gsreduce` IRAF task. Each reduced long-slit spectrum was then rectified to compensate for spectral curvature using the wavelength solution derived from the arc-spectra. Absolute flux-calibration was done by calibrating the spectral response function using a spectrophotometric standard star (G191B2B) observed as part of the observing project. Sky-subtraction is without doubt the largest uncertainty given the large number of unrelated sources in the vicinity (see Fig. 2), preventing us from isolating actual sky from background emissions. To isolate night-sky emission lines, we applied a median-filter along the spectral direction to isolate the smooth continuum from emission lines, and subtracted the latter from the rectified long-slit spectra, providing us with a line-free spectrum, but with night-sky and background continuum still intact. To extract the one-dimensional spectrum and finalize the sky-subtraction, we integrated the spectrum over the spatial extent

[1] Available from http://github.com/rkotulla/gmos-longslit

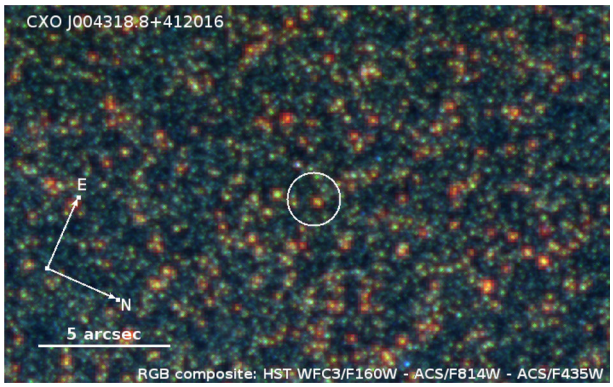

Figure 2. Composite figure of images in three filters of our target's field in the PHAT. Our optical target is the red and most luminous in the circle, which has a 1 arcsec diameter.

of the Hα emission line, and subtracted the scaled median of the direct vicinity along either side of the slit. The final spectrum, presented in Fig. 1, was then computed as the mean spectrum of all 10 individual spectra, rejecting outliers (e.g. remaining cosmics) via an iterative sigma-clipping algorithm.

We note that across the entire region covered by the slit we find weak Hα and [N II] emission, and cannot rule out a low-level contamination of the extracted spectra from unassociated background emission, in particular in the case of the weak [N II] detection. The slit was oriented with the parallactic angle, so the single exposures were taken at different hour angles, and in each of them the slit had a different orientation with respect to the sky coordinates. The emission lines we detected and measured were the same, and had the same characteristics, in each of the single exposures, so we are confident that the background and neighbourhood contamination is negligible, apart from the low flux level diffuse Hα and [N II] emission mentioned above. The emission spectrum we present here originates in our target star, the only one that was always in the slit.

Table 1. Emission lines in the optical spectrum of r3-8, and their flux, when measurable.

Line	Rest λ (Å)	Measured λ (Å)	Flux × 10^{-17} (erg s^{-1} cm^{-2})
H γ	4340.46	4335.84	2.83 ± 0.01
N III	4640.64	4634.7	
He II	4685.91	4679.99	4.21 ± 0.11
H β	4861.33	4855.55	10.89 ± 0.03
He I	4921.93	4916.76	3.83 ± 0.67
O [III]	5006.84	5000.51	3.09 ± 1.02
He I	5015.68	5010.55	2.49 ± 0.05
He I	5875.62	5868.69	7.31 ± 0.03
Na ID	5889.95	5883.42	1.54 ± 0.25
H α	6562.80	6555.05	72.99 ± 0.16
N [II]	6583.46	6575.31	1.98 ± 0.03
He I	6678.15	6669.85	6.18 ± 0.14
He I	7065.71	7056.69	10.35 ± 0.04

This spectrum is characterized by narrow, strong emission lines of the Balmer series, several He I lines and a relatively weak (compared to what we usually see in the hottest WD-symbiotics) He II line at 4686 Å. Lines due to very high excitation or ionization stages, like coronal lines, are missing in this source.

The measurements of the flux in the lines for the rest and measured wavelengths are shown in Table 1. The lines are blue-shifted by -349.8 ± 23.4 km s^{-1}, which is consistent with an object intrinsic in M 31. The systemic velocity of the galaxy is $\simeq -295$ km s^{-1} (Drout et al. 2009; McConnachie 2012). In the heliocentric velocity field measured by Emerson (1976), we find that the expected velocity is -240 ± 30 km s^{-1} at the star's location. Evans & Massey (2015) show that a difference of -90 km s^{-1} from the expected velocity is above the average, but it is not unusual at all for M31 red giants. We conclude that our object is in the thick disc or halo. We also note that foreground objects have positive velocity difference from the expected one, being blue-shifted by less than 150 km s^{-1}, so the velocity we measured proves M31 membership.

The emission lines are well detected in all the single exposures and in the median spectrum in Fig. 1, and we found no indication of clear variability of any of the lines' flux or line centres between different exposures.

Although the prominent Balmer lines in emission and the lines of neutral helium are typical of both Be stars and WD-symbiotics, our initial classification of the secondary as a B[e] star (Orio et al. 2015), due to the tentative identification of [Fe II] lines that are typical only of B[e] type stars, could not confirmed, in fact we found that those lines are not detected at a statistically significant level in the stacked spectrum.

The strong Balmer decrement (H α/H β = 6.7 and H γ/H β = 0.26) seems to imply high reddening; it would translate, in fact, into $E(B-V) = 0.71$ (or $A_V \simeq 2.2$ mag for a Galactic-type extinction law). We suggest that the Balmer decrement is due to high optical depth in the binary. The high extinction implies $N(H) \simeq 3.55 \times 10^{21}$ cm^{-2} (following Burstein & Heiles 1982), or $N(H) \simeq 3.94 \times 10^{21}$ cm^{-2} (following Predehl & Schmitt 1995), higher values than the best-fitting value in most X-ray observations and only marginally consistent with most X-ray spectra, although a 2015 exposure close to the Gemini observation indicates that $N(H)$ may have increased with respect to previous observations (see Section 4).

In the direction of M31 the interstellar absorption is very low, $E(B-V) \leq 0.07$ ($N(H) \simeq 3.50 \times 10^{20}$ cm^{-2} (following Burstein & Heiles 1982) or $\simeq 4.06 \times 10^{20}$ cm^{-2} (according to Predehl & Schmitt 1995), however the column density of neutral hydrogen inside M31 varies by a large factor. In Orio et al. (2010), we found a dust lane in the region of the source, and suggested that the SSS must be located in front of it, or else it would not have been detected. However, this is not necessarily so, considering accurate and spatially resolved data on dust extinction, recently published by Dalcanton et al. (2015). At the position of the source, in the maps of these authors we find $A_V \simeq 0.6$, corresponding to $E(B-V) \simeq 0.2$ and about $N(H) = 10^{21}$ cm^{-2} for a Galactic-type extinction law (however, the map shows large patchiness on very small scales, and there is much higher extinction in the zones neighbouring the source). Orio (2006) found also that the column density is likely to be variable, and that the 2σ lower limit in different observations is $N(H) \geq 9 \times 10^{20}$ cm^{-2} (which is consistent with $A_V \approx 0.6$). The variability may be due to an unstable wind, causing changing intrinsic absorption within the binary system. Orio (2006) also noted that the column density derived from the best fit increases, by up to a factor of 5, when the X-ray source is at maximum luminosity (thus the repeated X-ray dimming is not likely to be due to increased column density).

The emission line of He II at 4686 Å is often observed in WD-symbiotics (Luna & Costa 2005; Mikołajewska et al. 2017), and it is typical of supersoft X-ray sources. This line is often detected in many hot, accreting binaries, and it is always present in the spectra of accreting WDs. Because it is produced with a high ionization potential, it needs a hot environment and it usually originates near the WD. The flux in this line corresponds to a luminosity 3.7×10^{33} erg s^{-1} for the M31 distance, which is consistent with an accretion disc illuminated by ionizing radiation, coming from either the very massive hydrogen burning WD, or the disc itself if it surrounds a stellar mass black hole undergoing supercritical accretion with optically thick outflows. It is puzzling, however, that the ratio of the intensity of the He II and H β line is only 0.39, while usually in the other with hydrogen burning WDs, this ratio is about 1 (see e.g. SMC 3, AG Dra and Lin 358; Orio et al. 2007; Munari & Zwitter 2002). Also the ratio of the He I lines relative to H β is unusually large (He I λ5875/H $\beta \simeq 0.7$).

Because we cannot measure the continuum in the optical spectrum, in the next section we use archival data to analyse the nature of the secondary. Since we will show that it appears to be a red giant, we note here an interesting fact that constrains the spectral type: the absence of a TiO band, a feature that should have been measurable, suggests a classification of the red star as a giant of spectral type K or earlier.

We must also note the absence of the Raman scattering O VI line at 6825 Å, and of strong coronal lines of [Fe X], which were observed in the spectra of SMC 3 and other hydrogen burning WD-symbiotics (see Orio et al. 2007; Mikołajewska, Caldwell & Shara 2014). With a central source at a temperature close to a million K (see Section 4), the [Fe X] coronal line should have been produced in the optical spectrum unless the symbiotic nebular medium was much denser than in most symbiotic and the spectrum arises in a nebula with electron density above the critical one for this line, $n_e \simeq 5 \times 10^9$ cm^{-3} (Nagao et al. 2002).

3 THE NATURE OF THE SECONDARY AND THE FIT WITH AN ACCRETION DISC MODEL

Because we cannot reliably measure the continuum in our spectra due to the elevated sky background, we resorted to the photometric catalogs to examine the spectral energy distribution (SED) of our

Table 2. PHAT and LGS average magnitudes of the optical counterpart, as measured, and converted to absolute magnitude and dereddened assuming $E(B-V)=0.20$ (fourth column, mag$_a$1) and $E(B-V)=0.75$ (fifth column, mag$_a$2). The sixth column reports the actual measured magnitudes in the catalogs, and the LGS ones are accompanied by the average statistical error (seventh column) for the given filter; however, this is a lower limit for a crowded field. The statistical errors for the PHAT measurements are around 0.05 mag in relatively crowded fields like this one (Williams et al. 2014).

Filter	Center λ (Å)	Bandpass (Å)	mag$_{a1}$	mag$_{a2}$	mag	Δmag
F275W	2710	164.5	−3.372	−6.882	21.948	
F336W	3355	158.4	−4.53	−7.110	20.930	
U	3650	660	−3.376	−6.195	21.685	0.027
B	4450	940	−2.127	−4.187	23.133	0.10
F475W	4774	421.2	−2.533	−4.423	22.657	
V	5510	880	−2.527	−4.207	22.433	0.073
R	6580	1380	−3.017	−4.297	21.943	0.071
I	8060	1490	−3.819	−4.747	21.003	0.042
F814W	8030	663.3	−3.807	−4.759	21.001	
F110W	11 534	1427	−5.082	−5.582	19.578	
F160W	15 369	1341	−5.838	−6.168	18.732	

target from infrared (IR) to ultraviolet (UV). In Table 2 we give the magnitudes from the PHAT survey (Dalcanton et al. 2012; Williams et al. 2014; Johnson et al. 2015) as in the most recent version of the data release; these measurements supersede the values given in Chiosi et al. (2014), because an initial analysis of the Brick containing this object has been completed and revised by the PHAT team; see Williams et al. (2014). Additional measurements, albeit with a larger error, were obtained in the LGS (Local Group Survey; Massey et al. 2006) by stacking exposures taken in the course of over a year. The error bars in Table 2 are the mean errors of the LGS final photometry, but this field is sufficiently crowded to cause quite larger photometric errors. In Fig. 3 we show the PHAT co-added images of Brick 3, containing CXO J004318.8+412016, in the six PHAT filters, corresponding to the UV, optical UV, blue, optical IR and two IR bands (see Table 2).

There is a marginal, partial overlap of our target, encircled in green in the Figure and marked with 's', with stars 1 and 2 in the optical and IR filters. However, the PHAT indicates a quality flag of 'reliable' for the magnitudes measured for all the three objects; moreover, star 2 is measured to be at least 2 mag fainter than star 1 in all filters, and star 2 is about 3 mag fainter. We conclude that the crowding should not have affected the measurement in a very significant way, although the error may be larger than the average value in the PHAT.

Orbital modulations or other type of variability may make the photometric measurements less significant to derive the SED, because some of the PHAT images were obtained at different epochs. Our target was observed in field 9 of Brick 3 of the PHAT on 2013-07-15 in the *F275W*, *F336W* and *f160W* filters, on 2012-12-09 in the *F110W* filter, and in fields 8 and 9 on 2012-06-30 and 2012-07-01, respectively, in the *F814W* and *F475W* filters. In the LGS, for each filter the exposures were repeated on different dates in 2001 September and November and 2002 December. The photometry of this target can be done with a small error only by stacking the LGS images, so the catalog magnitudes in the Johnson filters are the average of 4–6 exposures. Orbital modulations are expected to occur on time-scales of the order of a year for a symbiotic, and of the order of several weeks for a Be binary. We examined the single LGS exposures in the single deep images obtained with the *U* filter and measured relative magnitudes, concluding that, even in exposures taken after about a year, there is no variability larger than 0.1 mag. The same is true for the two optical filters of the PHAT in which the exposure was repeated after 1 d. The several repeated LGS V and B exposures are quite shallow for this target, but we also examined them, finding no evidence of large variability. We do note that there is a difference of almost 1 mag between the two close wavelength ranges, that of filter *U* of the LGS and of filter *F336W* of the PHAT, so there may have been a large variation on a time-scale of 10 yr. However, it is likely that the colour indexes are relatively constant in each catalog, based on images obtained within little over a year, within possible fluctuations of ≈0.15 mag. We note that in Orio (2006) a WIYN telescope image was presented, in which our target was not detected with the blue filter, and an upper limit of $B<23.5$ was claimed, which would imply a variability amplitude of at least 0.36 mag. However, we checked the data again and found a typo in the caption; the upper limit for the detection was $B\simeq 22.5$ and the detected and measured star marked in the figure has $B\simeq 21.7$, not $B\simeq 22.7$.

In Fig. 4 we use the average PHAT magnitudes and colour indexes to show the position of the optical and UV object in the colour-magnitude diagrams. We examine two hypothesis, corresponding to two extreme values of $E(B-V)$, $E(B-V)=0.20$ indicated by the PHAT at the location of the source, and the value derived from Balmer decrement in the 2015 Gemini spectrum, $E(B-V)=0.71$. We remind that the range of column density evaluated from the [(albeit low signal to noise (S/N)] X-ray spectra is consistent with these two extremes, and it is likely to be variable. This is discussed more in Section 4.

CXO J004318.8+412016 has the colours of a young red giant, but there is an excess in the magnitudes measured with the Johnson *U* and *F336W* filter, whose bandpass is close to that of the *U*. First, we compared our object with evolutionary tracks of populations of different ages. The IR and optical colours of the optical counterpart are consistent with those a red giant of about 100 million years for the lower reddening value and the IR colours would indicate the helium burning loop, which is a short-lived phase, but not impossible to detect. The higher value of the reddening would imply a younger age of our source. The red component of SMC 3 is more luminous and consistent with an age of only 10 million years.

However, when we examine the U and UV colours, we find that the *HST* filter close to the *U* band places our target on the left of the evolutionary tracks (*F336W*–*F475W*). In the *U* filter there is no significant contamination of other nearby objects (stars 1 and 2, and other objects in the nearby fields, are not U bright, as Fig. 3 clearly shows). The reddening free value $Q=(U-B)-0.72(B-V)$, which is negative and around −1 for B star, has a very large value of $\simeq -1.9$ in the LGS, which is very unusual. We note that the *F275W*–*F336W* colour index is still consistent with a giant, although with a more luminous one, and of younger age (so young that seems to have been ruled out by the kinematics, which, as we mentioned, point at the thick disc or halo).

Our source is usually too faint for useful observations with the optical monitors of either *Swift* or *XMM–Newton*, it was out of their field of view in most exposures and in any case, source crowding and source confusion would also be problematic with these instruments. However, we note that no luminous UV sources with magnitude approximately lower than 21 were observed in this field with either the *Swift* optical monitor or *GALEX* (Orio et al. 2010), ruling out very large variability of CXO J004318.8+412016.

The largely negative *Q* value and the the high optical-UV flux are the reasons for which we initially suggested that the true optical counterpart may be a very young and massive Be star, which is a

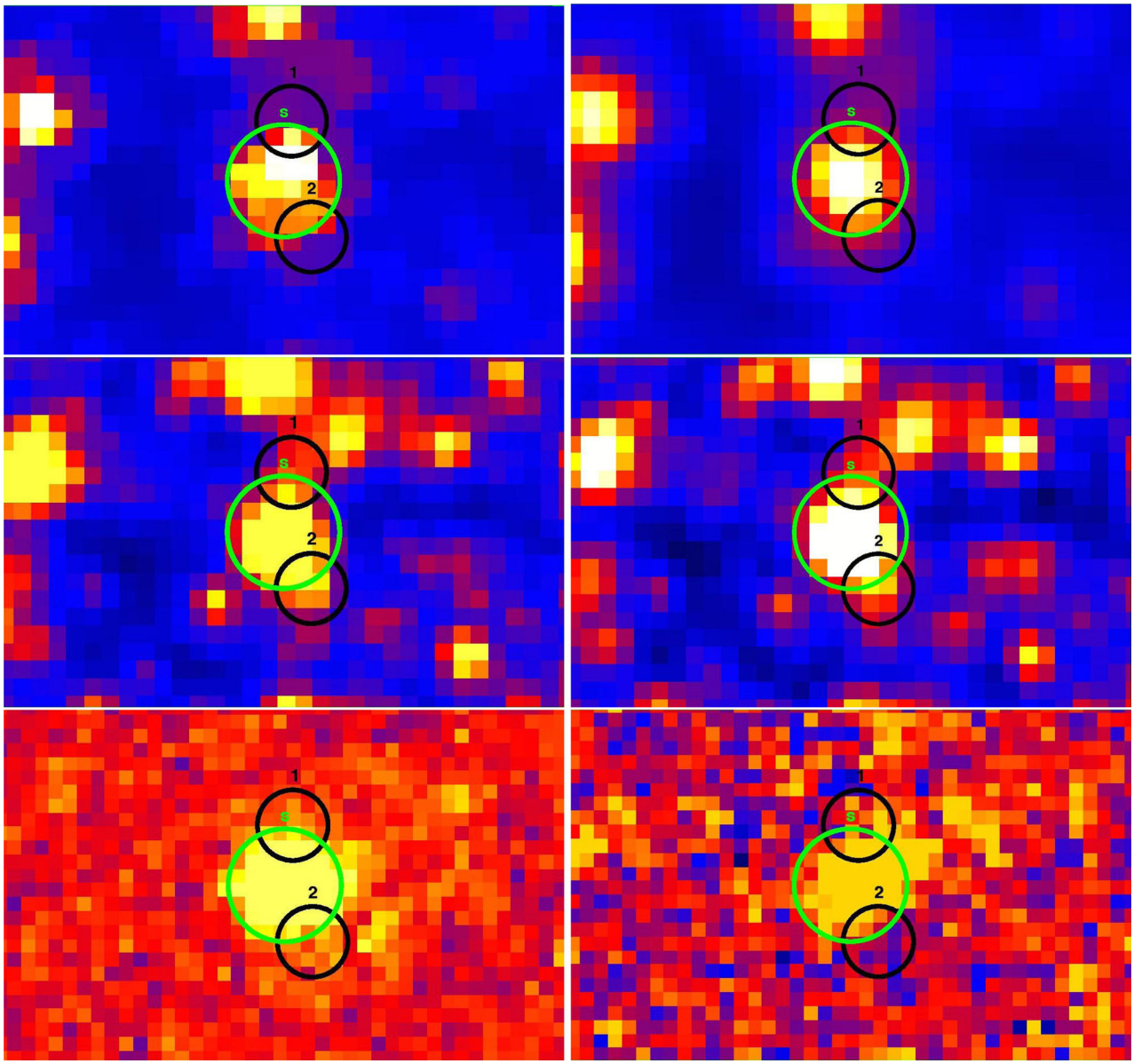

Figure 3. The field of CXO J004318.8+412016 around the star whose spectrum we are presenting, in the Brick 3 field of the PHAT, with the *F*110*W* filter (top left), *F*160*W* (top right), *F*814*W* (middle left), *F*475*W* (middle right), *F*336*W* (bottom left) and *F*275*W* (bottom right). Stars 1 and 2 are marked by a circle of 0.09 arcsec radius, and represent the two objects with overlapping wings of the PSF, measured in the PHAT (they are hardly detected in the IR and below threshold limits in the UV). Our target is in a 0.15 arcsec radius green circle. The images are oriented with North on top, and the field has dimensions of 1.6 × 1 arcsec.

possible classification based on the optical spectrum (Orio et al. 2015). However, we have shown here that the SED is *not* consistent with a Be star, but only with a red giant. Symbiotic stars were given their name because they present the spectral blend of a very hot (UV-emitting) and a luminous red object (a red giant or AGB, exceptionally perhaps a supergiant in case of a neutron star or black hole companion). The *U* luminosity in most cases is due to the symbiotic nebula, and possibly also to the accretion disc. However, the optical-UV luminosity (*U* and *F*336*W* filters) of CXO J004318.8+412016 seems to be unusually high with respect to the red band luminosity. The optical-UV flux cannot be attributed to the Raleigh–Taylor tail of the SSS, because the source temperature is so high, that 90 per cent of the bolometric luminosity would be emitted in X-rays, with about 10 per cent of the remaining flux in the extreme UV (see Orio et al. 2010).

In the first (upper left panel) of Fig. 5 we show that with a value $E(B-V) = 0.20$, consistently with Fig. 4, the optical colours are well fit with the SED of a red giant of 1 $M_\odot$, $T_{\rm eff}$ = 5300 K, and a radius of 43 $R_\odot$ (the same is true for the IR colours, as already demonstrated in Fig. 4). What causes the unusual excess in the UV bands? The possibility of an unresolved overlapping object contributing to the 'weird' optical-UV colour is very unlikely, given that it should be very luminous only in this band and not nearly as luminous in the nearby UV range. We also rule out a significant contribution of a symbiotic nebula, given that nebular lines are weak or absent.

We also compared the average magnitudes and colour indexes to a model of a disc in a binary, shown in the other panels of Fig. 5. We added an accretion disc to the SED of a secondary star, assuming both red and blue giants and varying the star's temperature

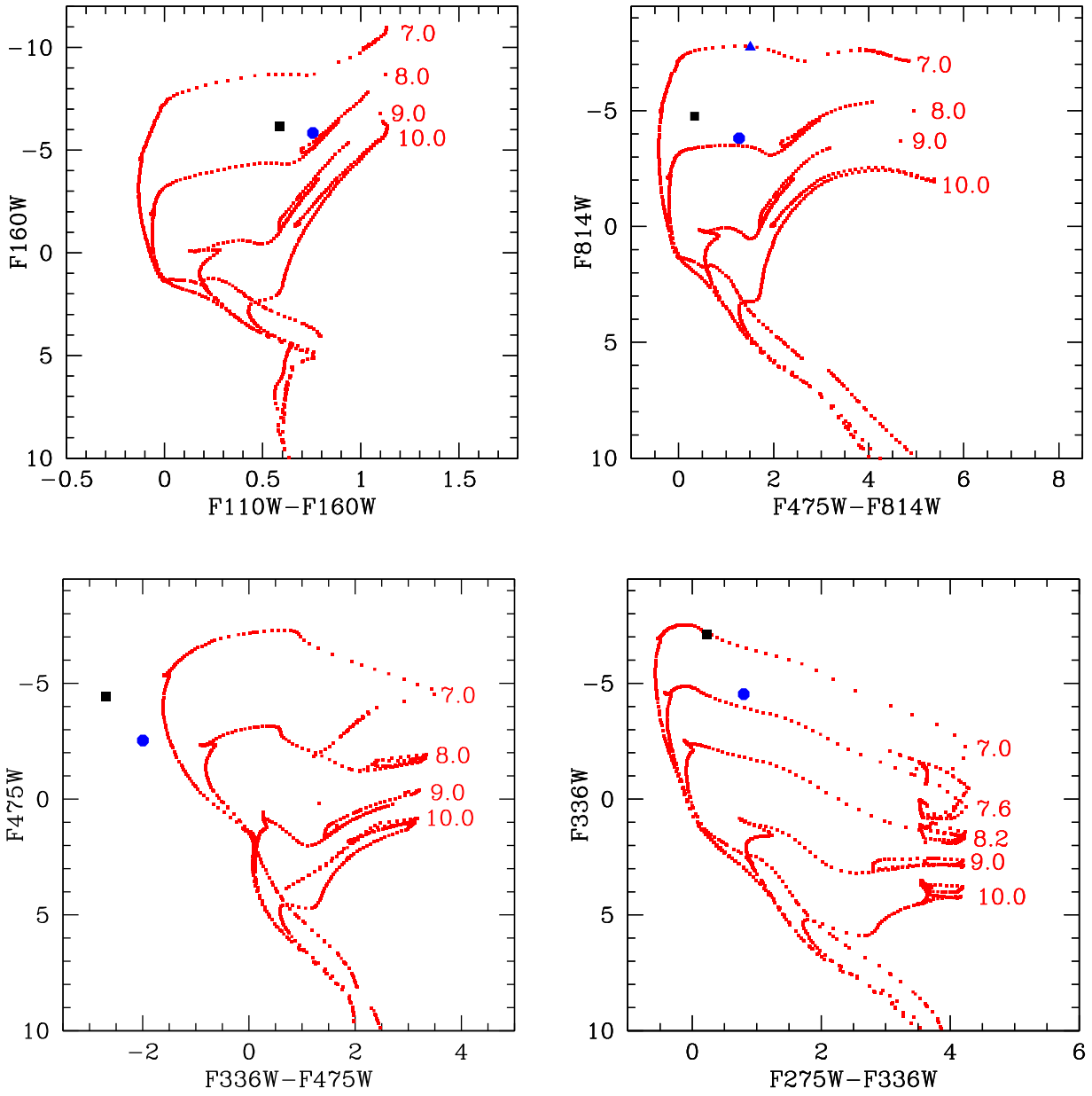

Figure 4. Color magnitude diagrams with isochrones of Bressan et al. (2012) and position of CXO J004318.8+412016. We assumed $E(B-V) = 0.20$ (blue circles) and $E(B-V) = 0.71$ (black squares) in dereddening the magnitudes. The triangle in the upper right panel indicates the position of SMC 3 in the diagram. The units are magnitudes on the *x*- and *y*-axis.

as a fitting parameter (of course, the presence of the disc implies a less luminous stellar component). The accretion disc was modelled, according to Patruno & Zampieri (2008). With this composite fit, we first ruled out that a B or other luminous main sequence star can be consistent with the SED of our object if we add a disc, because an accreting disc has a relatively flat spectral distribution. We show here the red giant+disc fits in the region from the *U* to *I* bands, the range of the spectrum included in the model by Patruno & Zampieri (2008), and in which we have an unusual SED. We performed several fits over a grid with different values of orbital periods, in each fit using the albedo and inclination as free parameters. The top right panel shows the fit adding to the red giant an accretion disc around a WD of 1.3 $M_\odot$, accreting from a 1 $M_\odot$ donor with a radius of 43 $R_\odot$ and $T_{\rm eff} = 4000$ K in a 90 d orbit, at inclination 80° and albedo = 0.8, and $E(B-V) = 0.20$. In all fits, we accounted also for irradiation of the secondary. In the bottom left panel, we found an approximate fit with a disc around a black hole of 5 $M_\odot$ from a donor star of 1 $M_\odot$, a radius of 30 $R_\odot$, temperature of 4000 K, inclination of 0°, albedo = 0.95 (bottom left panel) and $E(B-V)$ = 0.20 in a 60-d period (bottom left). Finally, in the bottom right panel we show the fit with a disc around a 1.3 $M_\odot$ WD with a companion of 1 $M_\odot$, $T_{\rm eff} = 4000$ K and a radius of 80 $R_\odot$ in a 230-d orbit, with inclination 0°, albedo = 0.5 and the higher absorption, $E(B-V) = 0.71$.

Assuming that the compact object is a WD, the disc hypothesis is quite consistent with the observed results, but there still is an excess towards the UV, which may be due to the Balmer jump in emission. Such a phenomenon is observed in about 33 per cent of symbiotics (Munari & Zwitter 2002; Henden & Munari 2008) although in the Galaxy only 4 WD-symbiotics show $U-B < -1$ (this is probably

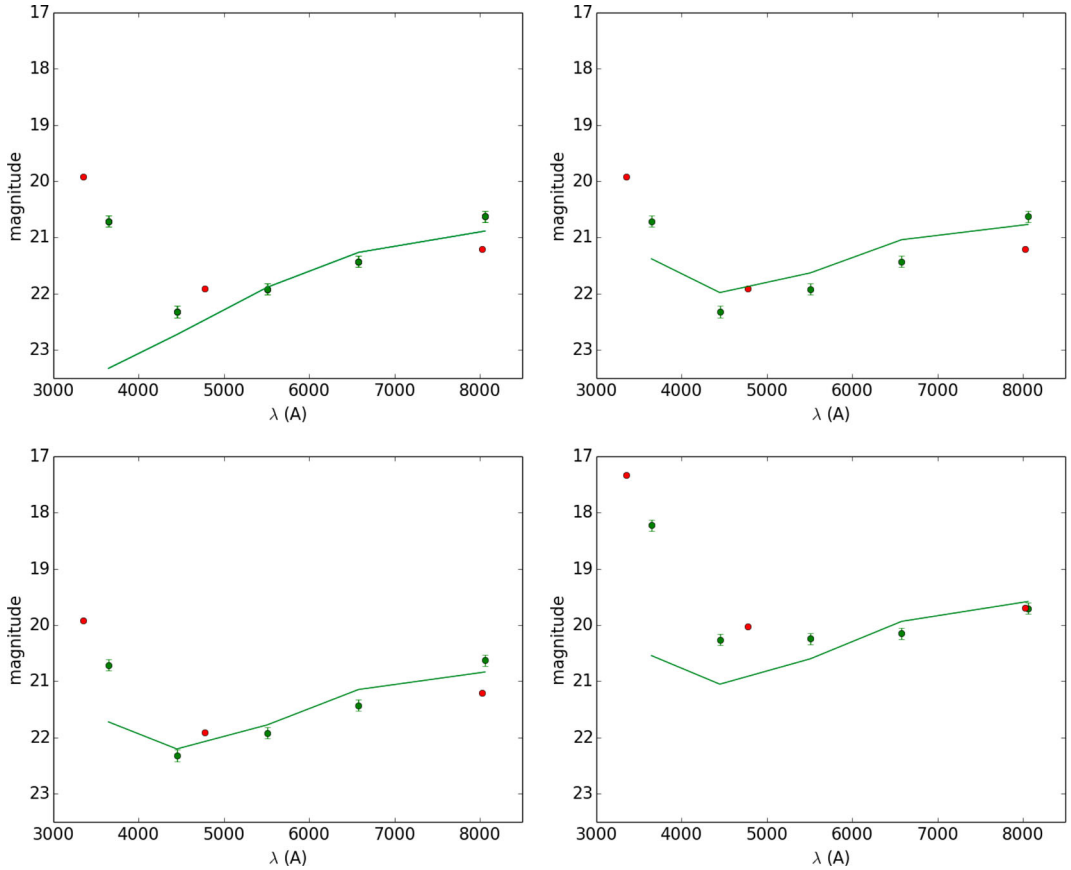

Figure 5. The green solid lines show the fit to the measured catalogs' magnitudes with a red giant (top left panel). The other panels show the fits by varying the red giant temperature and including an accretion disc: around a WD of 1.3 $M_{\odot}$ in the top right and bottom right panels with $E(B-V) = 0.20$ and $E(B-V) = 0.71$, respectively; around a black hole of 5 $M_{\odot}$ and $E(B-V) = 0.20$ in the bottom left panel (see the text for details). The LGS magnitudes are indicated by the green dots, and the PHAT ones by the red dots.

because most known Galactic symbiotics are affected by high reddening). The larger absorption, $E(B-V) = 0.71$ like we observed in our 2015 optical spectrum, is consistent with a low inclination, and with observing X-rays from a luminous central object (i.e. a WD). We caution that the disc model is calculated only assuming that the secondary fills its Roche lobe, which is not the case in several observed WD symbiotics, even those that show evidence of an accretion disc. This is the reason that the fit on the right-hand side of Fig. 5 is obtained with short orbital periods of 60 and 90 d, not observed in symbiotics, in which the average orbital periods are of the order of 2 yr (Belczyński et al. 2000; Mikołajewska 2012). Thus, these orbital periods should be regarded only as lower limits.

Accretion discs appear to be common in WD-symbiotics (see Nuñez et al. 2016, and references therein), although Kenyon & Gallagher (1983); Mikołajewska (2012), among others, have shown that the orbital separations of WD-symbiotics are too large for Roche lobe overflow, unless the secondary is deformed. Mikołajewska (2012) has pointed at the observed ellipsoidal variation of many WD-symbiotics as proof of disc formation in a modified Roche potential. In addition, discs in WD-symbiotics may be formed without Roche lobe overflow of the secondary, if the red giant wind carries angular momentum (similarly to the model of Huarte-Espinosa et al. 2013). Such a disc may be truncated and appear 'redder' than the standard disc we assumed in Fig. 5.

As shown in the bottom right panel of Fig. 5, the rise towards the UV cannot be explained at all with a disc around a black hole, while it seems marginally consistent with a disc around a WD. However, this is not a proof against the black hole hypothesis, because this part of the spectrum may contain a strong Balmer jump in emission. To summarize, the available photometric measurements do indicate quite clearly that the binary hosts red giant, but we do not have sufficient data to really rule out a black hole central object. The X-ray characteristics are more typical of hydrogen burning on a WD, but without high-resolution high energy spectra, which at present cannot be obtained yet at M31 distance, also the black hole cannot be ruled out. The solution may be given by measuring radial velocities of lines that may be emitted near the compact object.

4 THE X-RAY DATA IN THE LAST 15 YR

The field of CXO J004318.8+412016 was observed numerous times with *Chandra*, *XMM–Newton* and *Swift* in the last 15 years; however, many *Chandra*-ACIS observations and the vast majority of the *Swift* ones are too shallow for detection of the source, even in its high state. The upper limits through non-detections in X-ray observations are quite higher than actual measurements at minimum, so we do not include them in Table 3. It turns out that *XMM–Newton* can observe M31 only from the end of December to mid-February, and then again for a short period in the summer (July–August). As we reminded above, in Orio (2006), aspects of the the X-ray variability of the source were discussed and used the available data at that time; the column density did not seem to increase with

Table 3. In this table, available in electronic format, we give the count rates we derived for the *XMM–Newton* observations, first the ones done with EPIC-pn and the thin filter, then with EPIC-pn and the medium filter, both in the 0.2–1 keV and in the 0.2–1 keV ranges, and finally with EPIC-MOS and the medium filter in the 0.3–1 keV. The first column gives the modified Julian date, the second column gives the net exposure times (once the solar flares or other bad intervals were removed), the third the total duration of the exposure and Columns 4–6 list the count rates and their errors (see the text).

Julian Date	Net exp. (s)	Exp. (s)	cts s^{-1} (0.15–1 keV)	error(0.15–1)	cts s^{-1} (0.2–1 keV)	error(0.2–1)
			EPIC-pn, thin filter			
52281.28104167	55 330	64 317	1.039e-01	1.589e-03	5.767e-02	1.168e-03
53896.10890046	3831	21 913	5.507e-03	1.626e-03	6.826e-03	1.913e-03
54100.68317130	12 224	15 918	2.284e-02	2.388e-03	5.046e-02	3.192e-03

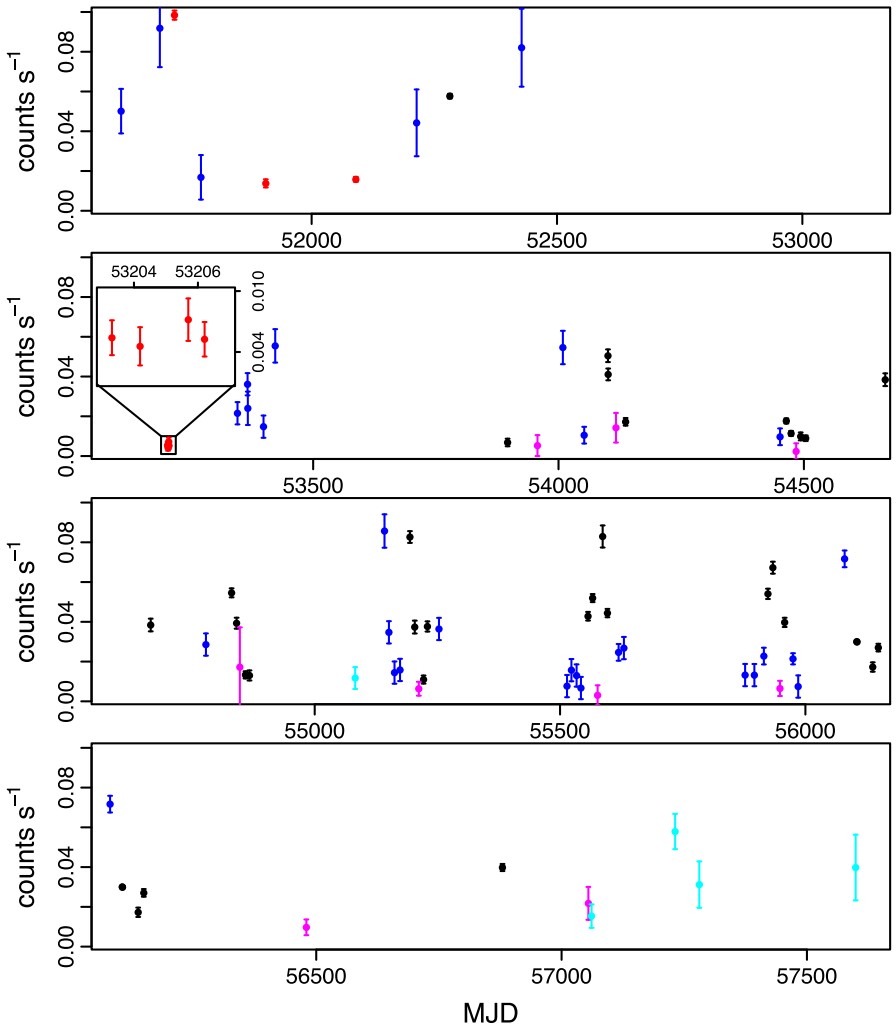

Figure 6. X-ray light curve obtained with *XMM–Newton* EPIC-pn and thin filter (black), EPIC-pn and medium filter (red), EPIC-MOS and the medium filter (purple), *Swift* XRT (light blue) and the *Chandra* HRC-I (blue). Because of lack of significant signal above 1 keV, in order to reduce the noise, the original count rates were extracted in the 0.2–1 keV range with EPIC-pn, in the 0.3–1 keV range for EPIC-MOS and *Swift* XRT. We used the count rates of the *Chandra* HRC-I from Hofmann et al. (2013) and converted all count rates in equivalent EPIC-pn thin filter count rate in the 0.2–1 keV range, assuming the model described in the text. The inset the second panel shows a zoom of observations obtained in four consecutive days, to show that the variability time-scale is longer than few days.

decreasing flux, but probably the opposite was true, suggesting that when the luminosity increases above a certain level, a depleting wind prevents the source from exceeding the Eddington luminosity.

The long-term X-ray light curve of CXO J004318.8+412016 is shown in Fig. 6, with the data obtained from the EPIC cameras of *XMM–Newton*, EPIC-pn with either the thin or medium filter and the MOS 1 and MOS 2 with the medium filter, and with the *Chandra* HRC-I, which is very sensitive in the very soft range. Finally, three significant *Swift* XRT detections were included for 2015–2016 (the previous *Swift* exposures were too short for a detection, or our source was at the very edge of the field). All the count rates have been converted to the EPIC-pn/thin-filter count rate in the 0.2–1 keV range (there are no significant counts above 1 keV), using the WebPIMMS online tool in HEASARC (FTOOL PIMMS v4.8b) and

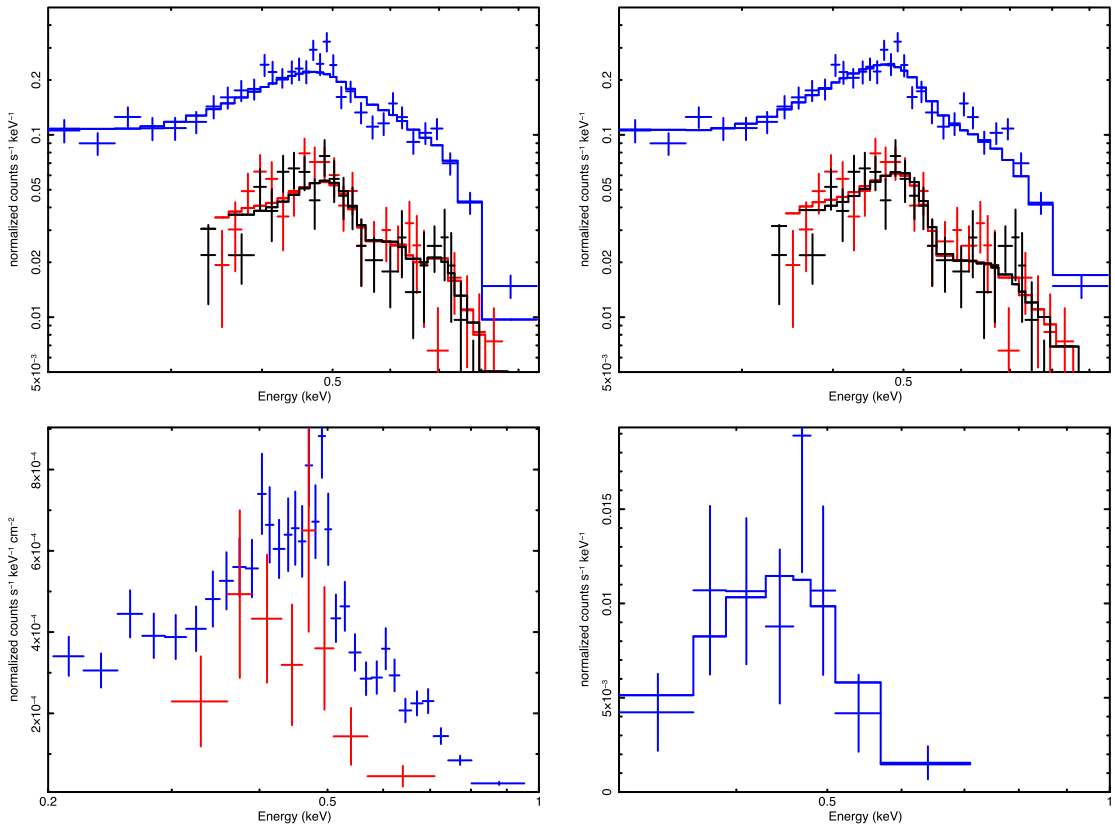

Figure 7. The upper panels show the count rate spectrum of the X-ray source observed with *XMM–Newton* EPIC-pn (blue) and with EPIC MOS-1 (black) and MOS-2 (red) on 2000 June 25 (these are the observations obtained with the highest S/N), and a fit with a WD atmospheric model on the left, with a blackbody on the right(see Table 4). In the lower panel on the left, we compare the EPIC-pn spectrum of 2000 June 25 with the Swift-XRT spectrum of the source observed on 2015 July 26, both convoluted with the effective area and thus plotted in units of counts s^{-1} cm^{-2} (left). On the bottom right panel, the Swift-XRT spectrum of the same date fitted with a blackbody, as in Table 4.

assuming a blackbody with a temperature of 70 eV and a column density $N(H) = 2 \times 10^{21}$ cm^{-2}, taken as average characteristics. As an indication, a count rate of 0.1 cts s^{-1} measured with EPIC-pn and the thin filter in the 0.2–10.0 keV range translates in an absorbed flux of 9.6×10^{-14} erg s^{-1} in the same range, with the above model. For this conversion we thus assumed the simplistic approximation that the spectrum does not vary, in order to give a term of comparison among the different instruments. In several observation the spectrum is measured at low S/N and there is a large uncertainty in the best-fitting parameters, so we looked for an approximate comparison and not an exact one. In any case, the flux fluctuations are much larger than uncertainties in the conversion between different observations and instruments, even with possible spectral variation.

Like in the observations done until 2005 (Orio 2006), we find that most observations indicate quite higher column density than between us and M31. In Fig. 7, we show fits with an atmospheric model to an observation done on 2000 June 25, one of the dates of largest X-ray flux of our source, and to an observation done on 2015 July 26, 15 yr later and close to the Gemini observation. Table 4, available online, reports all the count rates for the positive detections: the *XMM–Newton* ones were obtained with the *XMM – SAS* version 15.0.0 and its tool XSELECT, the *Swift* X-ray telescope (XRT) ones with the online tool of the UK Swift Data Center, while the *Chandra* HRC-I count rates were measured by Hofmann et al. (2013). There is no clear evidence that the spectrum softens in the lower states, although most of the low-luminosity observations are not of sufficient good quality to obtain statistically very meaningful spectral fits.

In Fig. 7 we show an example for a high X-ray flux period: fitting the observed spectrum in an *XMM–Newton* exposure of 2000 June 25 (observation 0112570401) with a blackbody indicates super-Eddington luminosity for a stellar mass of less than 4.9 $M_\odot$, at the 90 per cent confidence level. On the other hand, the fit to the spectrum with a WD atmospheric model (Rauch et al. 2010) indicates a luminosity of 7.1×10^{37} erg s^{-1} in the X-ray range, corresponding to more than 90 per cent the bolometric luminosity. Therefore, if the X-ray source is a nuclear burning WD, it is not emitting super-Eddington luminosity. We remind that a blackbody fit overestimates the luminosity and underestimates the temperature of a hydrogen burning WD atmosphere (see Rauch et al. 2010; Ness et al. 2011). The $T_{\rm eff}$ derived from the atmospheric fit is 86 eV, consistent with a WD mass between 1.2 and 1.3 $M_\odot$, according to Wolf et al. (2013).

We plotted the fit with the two different models in Fig. 7, and it is clear that it is very difficult to establish which one is more appropriate, even if the blackbody fit yields a lower value of χ^2, 1 versus 1.2. The atmospheric fit is much more complex and requires fine-tuning good-quality data, so we do not consider this as a proof that a blackbody is a much better fit, as expected if an accretion disc rather than an atmosphere is the origin of the X-rays. We also note that the fit to the 2015 data results in higher values of column density than in the 2000 observation, but given the uncertainties, this probably does not indicate a trend towards higher absorption over the years. In fact, the luminosity in the optical-UV band is

Table 4. Spectral parameters for the atmospheric and blackbody model, with the 90 per cent confidence level errors, and the χ^2 per degrees of freedom statistical parameter, during the exposure done with *XMM–Newton* on 2000 June 25 and with *Swift* on 2015 July 26. The net exposure time used to extract the spectrum was 22 250 s for the pn, 22 450 s for the two MOS and 18 250 s for the *Swift* XRT. L_X, absorbed and unabsorbed, is derived from the flux in the 0.2–1 keV range obtained in the fit, for a distance of 783 kpc or distance modulus 24.45 (Dalcanton et al. 2012). The error on the flux or luminosity is calculated assuming fixed $N(H)$ and $T_{\rm eff}$, and the luminosity is expressed in units of 10^{37} erg s^{-1}. The 90 per cent confidence level contours for the bolometric luminosity in the blackbody fit, and for the flux in the atmospheric fit, are unbound for the 2015 data.

	Atm. (2000)	Bbody (2000)	Atm. (2015)	Bbody (2015)
N(H) (10^{21} cm^{-2})	1.37 ± 0.21	$2.47^{+0.59}_{-0.24}$	$1.90^{+0.80}_{-0.17}$	$2.80^{+3.70}_{-1.90}$
$T_{\rm eff}$ (eV)	86 ± 4	67^{+3}_{-6}	67^{+60}_{-31}	46^{+30}_{-40}
$T_{\rm eff}$ (K)	$10^6 \pm 5 \times 10^4$	$7.78^{+0.4}_{-0.8} \times 10^5$	$7.74^{+7.74}_{-2.41} \times 10^5$	$5.34^{+3.47}_{-4.00} \times 10^5$
L (bol)	–	$61.3^{+80.3}_{-29.7}$	–	283.9
L_X (abs.)	$1.26^{+0.38}_{-0.28}$	–	0.43	–
L_X (unabs.)	$7.09^{+1.84}_{-1.56}$	–	5.55	–
χ^2	1.2	1.0	$\leq$1.0	$\leq$1.0

higher in the PHAT measurement obtained in 2013 than in the LGS images of 2001–2002, which argues against a long-term absorption increase.

Although with the data at hand we cannot rule out that the X-ray luminosity variations are aperiodic, there is a possibility that we are observing some kind of periodic obscuration due to a wind that is optically thick to soft X-rays and is observed only at a given orbital phase, like in the symbiotic star and supersoft X-ray source SMC 3 in the SMC (Orio et al. 2007; Sturm et al. 2011; Kato, Hachisu & Mikołajewska 2013). We detected no clear variability during the single exposures, neither between exposures repeated after few hours or a day (see inset in Fig. 5, showing exposures repeated for four consecutive days). We also rule out variability with an amplitude of more than $\simeq$15 per cent on time-scales of hours. Power spectra of the soft X-ray EPIC-pn light curve in the two longest observations (close to 7 h) done while the source was in a 'high' state revealed no significant peaks. There is also no evidence that the X-ray luminosity variation on time-scales of weeks may be due to an eclipse, because as we see in the inset of the second panel the low state can last for several days with a rather flat light curve, unlike for SMC3 (Kahabka 2004; Sturm et al. 2011) where there is a sharp drop and rise of flux. We cannot rule out also periodic modulations shorter than about 6 months and, probably, longer than about 3 weeks, because this is the time it takes for a dimming and re-brightening of the source in several *XMM–Newton* observations, with repeated fluctuations from the low to high state always repeated, even after several years. A *Swift* XRT exposure done in 2015 indicates high luminosity on 2015-14-09, very close in time to our Gemini exposures.

5 SOME CRUCIAL ASPECTS

The following puzzling characteristics of this source deserve further observations and related modelling:

(1) Given the high effective temperature of the X-ray source, coronal lines of [Fe X], especially the one at 6374 Å, which is very strong in the spectrum of SMC 3, should have been detected in the spectrum of CXO J004318.8+412016. If the X-rays are due to hydrogen burning, either hydrogen burning had temporarily been shut off when we observed it with Gemini, or CXO J004318.8+412016 is surrounded by much denser material than the symbiotics we know host a very hot WD. The electron density to avoid the [Fe X] forbidden transition is above a critical value of about 5×10^9 cm^{-3} (e.g. Nagao et al. 2002; Kato et al. 2013). We also note that the ratios of the intensity He I line at 6678 Å to those of the He I line at at 7065 Å or the He I triplet at 5876 Å indicate higher electron density than 10^7 cm^{-3}. Although this electron density appears to be higher than often observed in WD-symbiotics, this is not evidence against the WD presence. In fact all symbiotics, especially those with non-Mira donors, have at least some regions of high density. This is indicated, for instance, by their optical He I singlet to triplet ratios, [OIII] to H I line ratios, and UV intercombination line ratios. This fact is even used for distinguishing between symbiotic stars and planetary nebulae, like in the [OIII] diagnostic diagram used by Gutiérrez-Moreno, Moreno & Costa (1999), Mikołajewska et al. (2014) in the He I diagram of Proga, Mikolajewska & Kenyon (1994) and Mikołajewska et al. (2014).

(2) Another characteristic of the optical spectrum is the large Balmer decrement that we attribute to an optically thick medium. If it is due to intrinsic reddening in the binary, it indicates $E(B-V) \simeq 0.71$, more than three times higher than what we infer from the dust maps of Dalcanton et al. (2015). *Swift* XRT exposures-yielded detections were done within $\simeq$3 weeks before and after Gemini observations, but although the source may have varied within this time, the data are consistent with $N(H) \simeq 4 \times 10^{21}$ cm^{-2} and with the measured Balmer decrement. We stress that there is no simultaneous X-ray observation, but we know that the fit to the X-ray spectrum indicates that at least in many of the X-ray observations the value of the column density was lower. Will we observe a varying Balmer decrement if we take optical spectra at other epochs? It would be an interesting proof of variable absorption, due to a wind or other mass ejection phenomenon.

(3) The SED of this object is dominated by the presence of a red giant as the secondary. It is not an M giant, but of spectral type K or even earlier.

(4) Although we favour an explanation in terms of a hydrogen burning WD, a black hole primary cannot be ruled out yet with the existing data.

6 CONCLUSIONS

The prominent emission lines of the luminous object we observed in the narrow spatial error circle of CXO J004318.8+412016 are typical of the optical counterparts of X-ray binaries in general,

and of supersoft X-ray sources more specifically. According to the kinematics, it belongs to the M31 population. The continuum energy distribution from the IR to the UV is typical of an evolved star on the way to becoming a red giant, and the additional SED of an accretion disc only partially explains the rise of the flux towards the UV. This rise may be due to the Balmer jump in emission, which must be significant in a source with prominent Balmer lines.

The red giant SED that definitely suggests a symbiotic classification, but the optical spectrum presents several differences from those previously observed in a few other known hydrogen burning WD-symbiotics. Shell burning on a massive WD remains the most likely origin of the high supersoft luminosity in this source but we cannot rule out a black hole binary. The high optical depth and the likely possibility that the material from which the optical emission lines arise has electron density $n(\mathrm{e}) \geq 5 \times 10^9$ cm^{-3}, indicate significant intrinsic absorption. In the last 25 years, the absorption has been high and variable, although it was mostly not sufficiently high to absorb the supersoft X-rays of this very luminous source. It would be important to determine the precise time-scale of the X-ray variability and its possible periodicity. The X-ray light curve resembles the observed fluctuations known to occur in the X-ray luminosity of CAL 83, an SSS known as a WD burning binary, with a main sequence or slightly evolved secondary of higher mass than the WD (see Lanz et al. 2005). Measuring a period of the X-ray variability would also allow us to understand whether the X-ray source had shut off at the time the optical spectrum was taken: could this be the reason of the missing, or weak, emission lines due to high ionization or high excitation transitions? *Swift* XRT exposures about 3 weeks before and after the date on which almost all stacked spectra were obtained with Gemini, allowed us to measure a still active SSS. So, the time-scale for a temporary shut-off of the burning would be of the order of only few weeks.

The X-ray luminosity of CXO J004318.8+412016 oscillates between a few times 10^{35} erg s^{-1} and a few times 10^{37} erg s^{-1}, in the range of hydrogen burning WDs, as observed in post-outburst novae. We confirm that with the data at hand, it seems unlikely that this variation is related to changes in the absorption column. On the contrary, the variation of absorption column may be anti-correlated with the luminosity (Orio 2006). A tantalizing idea is that the supersoft X-ray luminosity variations indicate instead semi-degenerate thermonuclear flashes, repeated on time-scales of less than 3 months. When even a modest amount of material is ejected, the optical and X-ray luminosity increases, even if there is larger intrinsic absorption. In recent years, a nova has been observed to outburst in M31 with a recurrence period of less than a year (Henze et al. 2015; Darnley et al. 2016). With even shorter recurrence times, the flash is predicted to occur in only mildly degenerate conditions, with a luminosity increase of small amplitude compared with known classical novae, and almost without mass loss (see Fujimoto 1982; Wolf et al. 2013).

Although a very interesting group of SSS is found in young, massive binaries in the Magellanic Clouds (Orio 2013, and references therein), the majority of the persistent SSS we know are in symbiotic binaries. If the X-rays are due to hydrogen burning on a WD, because of the high $\dot{m}$ required for persistent burning, we can speculate that during the red giant phase of the secondary, some mechanism accelerates mass transfer. Also recurrent nova outbursts, which require high $\dot{m}$, but less than an order of magnitude than needed for steady burning (about 10^{-8} M$_\odot$ yr^{-1}) seem to be common in WD-symbiotics. 4 WD symbiotics that exploded as recurrent novae are known in the Galaxy, out of 16 known WD-symbiotics observed to undergo thermonuclear runaways (Mikołajewska 2012). Moreover, several observations indicate that surface hydrogen burning almost always occurs in the WDs of symbiotic systems (Mikołajewska 2012, and references therein). Luna et al. (2013) found a fraction of symbiotics with no detectable fast UV variability, suggesting that their luminosity is powered by nuclear burning on low-mass WDs.

These facts have made WD-symbiotic appear very interesting as SNe Ia progenitors as single degenerate binaries. However, proving or ruling out that they are a significant channel to SNe Ia while they are still single degenerate systems (we note that double degenerates also need to have a symbiotic evolutionary phase), requires much better statistics than we currently have. The SSS would only rarely be detectable, because of the large intrinsic absorption of the symbiotic's nebula and wind, so the observed SSS are only the ones effected by low absorption, that is, the tip of the iceberg. The sample of SSS WD-symbiotics in nearby galaxies includes one likely symbiotic nova, RX J0550.0-7151 (Schmidtke & Cowley 1995; Charles, Southwell & O'Donoghue 1996) and three persistent sources, SMC 3, Lin 358 and Draco C-1, the last two at low $T_{\mathrm{eff}} \leq 200\,000$ K. We now have the means to study symbiotics at large distances in the Local Group. Mikołajewska et al. (2014) have identified 35 symbiotics in Andromeda, Gonçalves et al. (2006) discovered one in IC 10 (2008), Gonçalves et al. (2015) presented a symbiotic and two additional candidates in NGC 205 and Kniazev et al. (2009) discovered 1 in NGC 6822, and 12 are known in M33 (Mikołajewska et al. 2017). These objects were found through Hα imaging. Due to the detection limits, we estimate that they probably represent only the 20 per cent most optically luminous symbiotics at $\simeq$800 kpc distance. Several authors noticed that they mostly have AGB companions.

We suggest that coordinated X-ray and optical observations of CXO J004318.8+412016 should be done in the near future. First of all, it would be important to follow the variations of optical depth and/or intrinsic absorption (from the optical spectrum) and column density $N(H)$, assessing whether they are correlated. Other than the temporary shut-off of the burning, there is a possibility that the emission lines corresponding to the transitions with the highest ionization potential were not observed in the optical spectrum because of a peculiar geometry and distribution of the absorbing gas in the system. Ultimately, it would be extremely interesting for the evolutionary models to understand whether the brightening and dimming of the source are due to a nova-like phenomenon: this would be a very fast recurrent nova of very small amplitude, possibly an only mildly degenerate thermonuclear runaway, without mass outflow.

Another important set of observations should aim at the measurement of the radial velocity displacement of the emission lines that may be produced near the compact object, so with some assumption we should be able to estimate the mass of the compact object, and assess whether it is indeed a massive WD. We are still unable to rule out another interesting possibility for the nature of the object, that of a black hole binary. Spectroscopic monitoring over a few years may reveal radial velocity displacements of the emission lines, which will be crucial to assess the nature of this 'extreme' and intriguing X-ray source.

ACKNOWLEDGEMENTS

G. Juan Luna is a member of the CIC-CONICET and his work was supported by grant Pip-Conicet/2011 #D4598, ANPCYT-PICT 0478/14. Ralf Kotulla gratefully acknowledges financial support from the National Science Foundation under Grants No. 1412449 and No. 1664342. Joanna Mikolajewska acknowledges support of the Polish National Science Centre grant

DEC-2013/10/M/ST9/00086, and Domitilla de Martino of ASI-INAF Grant No. I/037/12/0.

REFERENCES

Barnard R., Garcia M. R., Primini F., Li Z., Baganoff F. K., Murray S. S., 2014, ApJ, 780, 83
Belczyński K., Mikołajewska J., Munari U., Ivison R. J., Friedjung M., 2000, A&AS, 146, 407
Bressan A., Marigo P., Girardi L., Salasnich B., Dal Cero C., Rubele S., Nanni A., 2012, MNRAS, 427, 127
Burstein D., Heiles C., 1982, AJ, 87, 1165
Charles P. A., Southwell K. A., O'Donoghue D., 1996, IAU Circ., 6305
Chiosi E., Orio M., Bernardini F., Henze M., Jamialahmadi N., 2014, MNRAS, 443, 1821
Dalcanton J. J. et al., 2012, ApJS, 200, 18
Dalcanton J. J. et al., 2015, ApJ, 814, 3
Darnley M. J. et al., 2016, ApJ, 833, 149
Drout M. R., Massey P., Meynet G., Tokarz S., Caldwell N., 2009, ApJ, 703, 441
Emerson D. T., 1976, MNRAS, 176, 321
Evans K. A., Massey P., 2015, AJ, 150, 149
Evans P. A. et al., 2013, VizieR Online Data Catalog, 9043
Fujimoto M. Y., 1982, ApJ, 257, 767
Gonçalves D. R., Ercolano B., Carnero A., Mampaso A., Corradi R. L. M., 2006, MNRAS, 365, 1039
Gonçalves D. R., Magrini L., de la Rosa I. G., Akras S., 2015, MNRAS, 447, 993
Gutiérrez-Moreno A., Moreno H., Costa E., 1999, PASP, 111, 571
Henden A., Munari U., 2008, Baltic Astron., 17, 293
Henze M. et al., 2014a, A&A, 563, A2
Henze M., Ness J.-U., Darnley M. J., Bode M. F., Williams S. C., Shafter A. W., Kato M., Hachisu I., 2014b, A&A, 563, L8
Henze M., Darnley M. J., Kabashima F., Nishiyama K., Itagaki K., Gao X., 2015, A&A, 582, L8
Hofmann F., Pietsch W., Henze M., Haberl F., Sturm R., Della Valle M., Hartmann D. H., Hatzidimitriou D., 2013, A&A, 555, A65
Huarte-Espinosa M., Carroll-Nellenback J., Nordhaus J., Frank A., Blackman E. G., 2013, MNRAS, 433, 295
Johnson L. C. et al., 2015, ApJ, 802, 127
Kaaret P., 2002, ApJ, 578, 114
Kahabka P., 2004, A&A, 416, 57
Kato M., Hachisu I., Mikołajewska J., 2013, ApJ, 763, 5
Kenyon S. J., Gallagher J. S., 1983, AJ, 88, 666
Kniazev A. Y. et al., 2009, MNRAS, 395, 1121
Lanz T., Telis G. A., Audard M., Paerels F., Rasmussen A. P., Hubeny I., 2005, ApJ, 619, 517
Liu J., 2011, ApJS, 192, 10
Liu J.-F. et al., 2015, Nature, 528, 108
Luna G. J. M., Costa R. D. D., 2005, A&A, 435, 1087
Luna G. J. M., Sokoloski J. L., Mukai K., Nelson T., 2013, A&A, 559, A6
Massey P., Olsen K. A. G., Hodge P. W., Strong S. B., Jacoby G. H., Schlingman W., Smith R. C., 2006, AJ, 131, 2478
McConnachie A. W., 2012, AJ, 144, 4
Meng X. C., Yang W. M., 2011, A&A, 531, A94
Mikołajewska J., 2012, Baltic Astron., 21, 5
Mikołajewska J., Caldwell N., Shara M. M., 2014, MNRAS, 444, 586
Mikołajewska J., Shara M. M., Caldwell N., Iłkiewicz K., Zurek D., 2017, MNRAS, 465, 1699
Munari U., Zwitter T., 2002, A&A, 383, 188
Nagao T., Murayama T., Shioya Y., Taniguchi Y., 2002, ApJ, 575, 721
Ness J.-U. et al., 2011, ApJ, 733, 70
Nuñez N. E., Nelson T., Mukai K., Sokoloski J. L., Luna G. J. M., 2016, ApJ, 824, 23
Orio M., 2006, ApJ, 643, 844
Orio M., 2012, BAAS, 40, 333
Orio M., 2013, Astron. Rev., 8, 010000
Orio M., Zezas A., Munari U., Siviero A., Tepedelenlioglu E., 2007, ApJ, 661, 1105
Orio M., Nelson T., Bianchini A., Di Mille F., Harbeck D., 2010, ApJ, 717, 739
Orio M., Luna G. J. M., Kotulla R., Gallagher J. S. G., 2015, Astron. Telegram, 8204
Osborne J. P., 2015, J. High Energy Astrophys., 7, 117
Patruno A., Zampieri L., 2008, MNRAS, 386, 543
Pietsch W., Freyberg M., Haberl F., 2005, A&A, 434, 483
Pietsch W., Fliri J., Freyberg M. J., Greiner J., Haberl F., Riffeser A., Sala G., 2006, A&A, 454, 773
Predehl P., Schmitt J. H. M. M., 1995, A&A, 293, 889
Proga D., Mikolajewska J., Kenyon S. J., 1994, MNRAS, 268, 213
Rauch T., Orio M., Gonzales-Riestra R., Nelson T., Still M., Werner K., Wilms J., 2010, ApJ, 717, 363
Rosen S. R. et al., 2016, A&A, 590, A1
Schmidtke P. C., Cowley A. P., 1995, IAU Circ., 6278
Starrfield S., Timmes F. X., Iliadis C., Hix W. R., Arnett W. D., Meakin C., Sparks W. M., 2012, Baltic Astron., 21, 76
Sturm R. et al., 2011, A&A, 529, A152
Trinchieri G., Fabbiano G., 1991, ApJ, 382, 82
Wang S., Qiu Y., Liu J., Bregman J. N., 2016, ApJ, 829, 20
Williams B. F. et al., 2014, ApJS, 215, 9
Wolf W. M., Bildsten L., Brooks J., Paxton B., 2013, ApJ, 777, 136

SUPPORTING INFORMATION

Supplementary data are available at *MNRAS* online.

Table3.txt

Please note: Oxford University Press is not responsible for the content or functionality of any supporting materials supplied by the authors. Any queries (other than missing material) should be directed to the corresponding author for the article.

This paper has been typeset from a TEX/LATEX file prepared by the author.